JACS
JOURNAL OF THE AMERICAN CHEMICAL SOCIETY
pubs.acs.org/JACS
Article

Designer "Quasi-Benzyne": The Spontaneous Reduction of Ortho-Diiodotetrafluorobenzene on Water Microdroplets

Huan Chen,[‖] Ruijing Wang,[‖] Tatsuya Chiba,[‖] Kathryn Foreman, Kit Bowen,* and Xinxing Zhang*

Cite This: J. Am. Chem. Soc. 2024, 146, 10979−10983
Read Online
ACCESS | Metrics & More | Article Recommendations | Supporting Information

ABSTRACT: It has been widely shown that water microdroplets have a plethora of unique properties that are highly distinct from those of bulk water, among which an especially intriguing one is the strong reducing power as a result of the electrons spontaneously generated at the air−water interface. In this study, we take advantage of the reducing power of water microdroplets to reduce ortho-diiodotetrafluorobenzene (o-$C_6F_4I_2$) into a $C_6F_4I_2^{\bullet-}$ radical anion. Photoelectron spectroscopy and density functional theory computations reveal that the excess electron in $C_6F_4I_2^{\bullet-}$ occupies the I−C1−C2−I linkage, which elongates the C−I bonds but surprisingly shortens the C1−C2 bond, making the bond order higher than a double bond, similar to the benzyne molecule, so we named it "quasi-benzyne". The $C_6F_4I_2^{\bullet-}$ anion was further successfully utilized in a Diels−Alder reaction, a typical reaction for benzyne. This study provides a good example of strategically utilizing the spontaneous properties of water microdroplets and generating an especially exotic anion, and we anticipate that microdroplet chemistry can be an avenue rich in opportunities for new catalyst-free organic reactions.

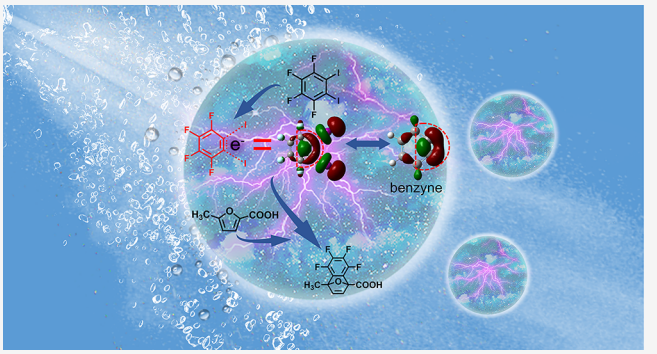

1. INTRODUCTION

Over the past few years, water microdroplet chemistry has emerged as a new paradigm of research for its exceptional ability to significantly accelerate chemical reactions by several orders of magnitude, outpacing the same reactions that occur in bulk water.[1,2] What's more remarkable is that microdroplets can sometimes trigger reactions that cannot occur in the bulk.[3−5] It is been widely accepted that microdroplets accelerate chemical reactions via various mechanisms,[1,6−13] including partial solvation, extreme pH conditions, and ultrahigh electric fields. Among these mechanisms, the spontaneous generation of an ultrahigh electric field (10^9 V/m) on the surface of microdroplets is particularly fascinating. Such a high electric field at the microdroplet surface can even split the hydroxide ions (OH^-) in water into hydroxyl radicals ($^{\bullet}OH$) and electrons,[8,9] making the microdroplets both oxidative and reductive.[14] In this study, we focus on only the reducing power of microdroplets. Existing studies involve the reduction of pyridine into pyridyl anion,[15] the reduction of chloroauric acid in aqueous solution into gold nanoparticles and nanowires,[16] the reduction of doubly charged viologens into singly charged radicals,[17] the reduction of water into H_2,[18] the reduction of transition metal ions,[19] as well as the reduction of iodopentafluorobenzene to its parent anion radicals.[20] A more comprehensive overview of the redox capabilities can be found in a literature review.[14] The electric field on microdroplets could result from the alignment of the free O−H bonds of the interfacial water molecules.[21] Other studies have proposed that the formation of electric double layers might cause the high electric field.[22]

In this study, we extend the reducing ability of microdroplets to the ortho-diiodotetrafluorobenzene ($C_6F_4I_2$) molecule. The parent radical anion, $C_6F_4I_2^{\bullet-}$, was observed. This anion is exotic because the excess electron dwells on the I−C1−C2−I linkage, and it weakens both of the C−I bonds but strengthens the C1−C2 bond, making it resemble the benzyne molecule (C_6H_4), which has a C1−C2 triple bond (vide infra). As a result, we name the $C_6F_4I_2^{\bullet-}$ radical anion "quasi-benzyne". This quasi-benzyne was further utilized in a Diels−Alder (DA) C−C cycloaddition reaction, a typical reaction that real benzyne is often utilized for.[23] C−C cycloaddition is important in synthetic chemistry, facilitating modular accesses to the synthesis of natural products,[24,25] agrochemicals,[26] and pharmaceuticals.[27,28] Among the cycloaddition reactions, the DA reaction between a diene and a dienophile is well-known for its regioselectivity and stereoselectivity. DA reactions usually require catalysts such as Lewis acids,[29,30] alkali cations,[31] and enzymes.[32] Recently, using strong external

Received: February 25, 2024
Revised: March 27, 2024
Accepted: March 28, 2024
Published: April 8, 2024

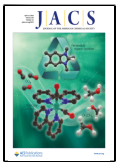

https://doi.org/10.1021/jacs.4c02819
J. Am. Chem. Soc. 2024, 146, 10979−10983

electric fields to catalyze DA reactions has also emerged as a new method.[33−35] In this study, we achieved the DA reaction between the quasi-benzyne $C_6F_4I_2^{\bullet-}$ and a furan-based diene in microdroplets, based on which we anticipate that microdroplet chemistry can provide a new pathway rich in opportunities for catalyst-free DA reactions.

2. RESULTS AND DISCUSSION

Detailed experimental methods are provided in the Supporting Information (SI). Figure 1a illustrates the setup of the

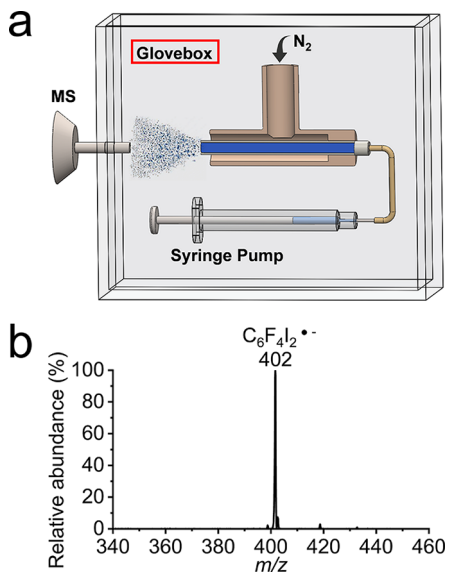

Figure 1. Spontaneous reduction of $C_6F_4I_2$ in water microdroplets. (a) Experimental setup of the sprayer in a glovebox filled with pure N_2. (b) Typical mass spectrum showing the spontaneous reduction products, $C_6F_4I_2^{\bullet-}$.

microdroplet experiment in a glovebox filled with N_2. The inlet of the mass spectrometer is inserted into the glovebox in an airtight manner for analysis purposes.[36] A $C_6F_4I_2$ aqueous solution was forced by a syringe pump through a fused silica capillary that sits inside a larger coaxial capillary through which high-pressure N_2 sheath gas flows. The resulting spray of microdroplets is aligned with the inlet of the mass spectrometer operated in the negative mode of detection. The distance between the outlet of the sprayer and the mass spectrometer inlet is the flying distance of the microdroplets, which defines the microdroplet reaction time. Figure 1b presents a typical and clean mass spectrum of the $C_6F_4I_2^{\bullet-}$ parent anion at m/z = 402. It originates from the spontaneous reduction of $C_6F_4I_2$ by an electron, supporting the notion that electrons are readily available on microdroplets. The same experiment was carried out in the atmosphere, and the signal of $C_6F_4I_2^{\bullet-}$ was notably lower than that in the glovebox, attributed to the oxidative nature of air.[19] The collision-induced dissociation (CID) spectrum was used to confirm the structure of $C_6F_4I_2^{\bullet-}$ (Figure S1).

In order to obtain insights into the geometric and electronic structures of $C_6F_4I_2^{\bullet-}$, gas-phase photoelectron spectroscopy (PES) measurements and density functional theory (DFT) calculations were performed. A comprehensive description of the methods is in the SI. Briefly, a home-built apparatus combines a laser photoemission ion source, time-of-flight (TOF) mass spectrometry, and anion PES. We analyzed the kinetic energies of the resultant photoelectrons by crossing a mass-selected anion beam with a 266 nm laser beam. The energetics of the photodetachment process are governed by $h\nu$ = EBE + EKE, where $h\nu$ is the photon energy, EBE is the electron binding (photodetachment transition) energy, and EKE is the electron kinetic energy. As illustrated in Figure 2a,

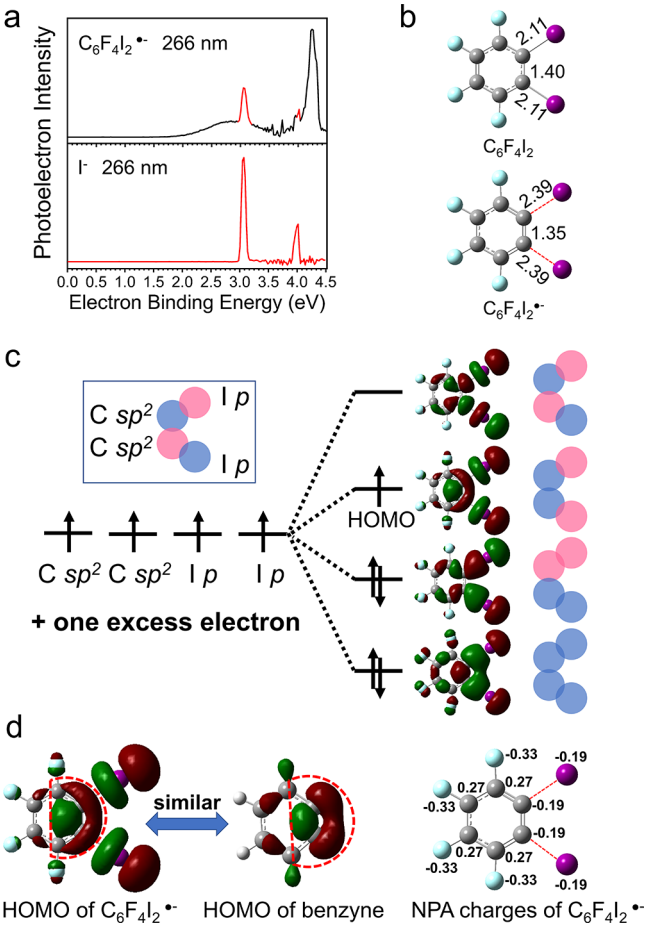

Figure 2. Photoelectron spectroscopic and DFT studies of $C_6F_4I_2^{\bullet-}$. (a) Spectra of $C_6F_4I_2^{\bullet-}$ and I^-. (b) Calculated structures of neutral and anionic $C_6F_4I_2$. (c) Correlation diagram of the frontier orbitals of $C_6F_4I_2^{\bullet-}$ from the combinations of two carbon sp^2 orbitals and two iodine p orbitals. (d) Resemblance between the HOMOs of $C_6F_4I_2^{\bullet-}$ and benzyne, and the NPA charges of $C_6F_4I_2^{\bullet-}$.

the spectrum of $C_6F_4I_2^{\bullet-}$ exhibits an EBE band starting from around 1.80 eV and peaking at 2.84 eV, these two values correspond to the electron affinity (EA) of $C_6F_4I_2$ and vertical detachment energy (VDE) of $C_6F_4I_2^{\bullet-}$, in good consistency with our calculated values, 1.77 and 3.01 eV, at the B3LYP/aug-cc-pVTZ(C,F,H,O)/aug-cc-pVTZ-PP(I) level of theory (Table 1). The second EBE band peaking at 4.24 eV corresponds to the transition from the anion to the excited

Table 1. Experimental and Theoretical EA and VDE Values Are Given in eV[a]

species	expt. EA	theo. EA	expt. VDE	theo. VDE
$C_6F_4I_2$/ $C_6F_4I_2^{\bullet-}$	1.80	1.77	2.84	3.01
I/I^-	3.06[37]			

[a]The calculations were performed at the B3LYP/aug-cc-pVTZ-(C,F,H,O)/aug-cc-pVTZ-PP(I) level of theory.

https://doi.org/10.1021/jacs.4c02819
J. Am. Chem. Soc. 2024, 146, 10979−10983

state of the neutral, which is also in good agreement with the calculated value, 4.42 eV. The spectrum of I^- in Figure 2a shows a sharp peak at 3.06 eV, corresponding to the well-known EA of iodine.[37] The $C_6F_4I_2^{\bullet-}$ spectrum obviously has features from I^- (red), which is a result of a two-photon process: the first photon dissociates $C_6F_4I_2^{\bullet-}$ into C_6F_4I and I^-, and the second photon photodetaches I^-.

Figure 2b shows the calculated structures of $C_6F_4I_2$ and $C_6F_4I_2^{\bullet-}$. The two C−I bonds are elongated from 2.11 Å in the neutral to 2.39 Å in the anion. This result is consistent with a previous study, where the $C_6F_4I_2^{\bullet-}$ anion was generated and imaged by scanning tunneling microscopy.[38] This large bond length change is also consistent with the observed wide EBE band in the PES as a result of the poor Franck−Condon overlap. However, the C1−C2 bond length is shortened from 1.40 Å in the neutral orbital to 1.35 Å in the anion, which is surprising, because an excess electron often weakens a chemical bond by occupying the antibonding orbital. From merely the bond length change, one can already see $C_6F_4I_2^{\bullet-}$ has some benzyne character, since the latter has a metastable C1−C2 triple bond (1.22 Å), which is shorter than the other C−C bonds in the benzyne skeleton (~1.4 Å). The Cartesian coordinates of all of the calculated species are provided in Table S1.

To better understand the unusual C1−C2 bond length in $C_6F_4I_2^{\bullet-}$, we further calculated its frontier molecular orbitals (MOs), which can be regarded as combinations from the sp^2 orbitals of the two carbon atoms and the p atomic orbitals of the two iodine atoms (Figure 2c). The sp^2 orbitals and p orbitals are also simplified as pink and blue circles in Figure 2c, and the two colors represent opposite parities. In the highest occupied molecular orbital (HOMO) of $C_6F_4I_2^{\bullet-}$, which is also a singly occupied molecular orbital (SOMO), the excess electron is delocalized on the I−C1−C2−I linkage, which is actually a combination of two C−I σ^* antibonding orbitals between the sp^2 orbitals of the two carbon atoms and the p orbitals of the two iodine atoms, and a C1−C2 π bonding orbital between the sp^2 orbitals of the two carbon atoms. As a result, we have confirmed a very interesting phenomenon: one electron changes three bonds in opposite directions, the C1−C2 bond shortens, but the C−I bonds elongate.

Figure 2d presents a comparison between the HOMOs of $C_6F_4I_2^{\bullet-}$ and benzyne (C_6H_4). The circled parts in the two HOMOs are similar, corresponding to the π bonding characters between the two carbon atoms. The overlap of the π bond is not perfect, making this bond highly reactive. The C1−C2 bond order of benzyne, which is regarded as three, must be higher than that of $C_6F_4I_2^{\bullet-}$ because the HOMO of $C_6F_4I_2^{\bullet-}$ only has one electron, and only part of this electron localizes between the two carbon atoms. This explains that the C1−C2 bond length in $C_6F_4I_2^{\bullet-}$ (1.35 Å) is longer than that of benzyne (1.22 Å), but shorter than that of the neutral $C_6F_4I_2$ (1.40 Å). Natural population analysis (NPA) of $C_6F_4I_2^{\bullet-}$ provides the charge of each atom (Figure 2d). Not surprisingly, C1 and C2 are negatively charged by −0.19 e even though carbon is the most electropositive element in this molecule. The other carbon atoms are positively charged. Taken together, we name $C_6F_4I_2^{\bullet-}$ a "quasi-benzyne", for its C1−C2 bond order is more than a benzene molecule so that it can possess some benzyne character.

A benzyne molecule readily reacts with a diene as a dienophile in DA reactions.[23] To further confirm the benzyne feature of $C_6F_4I_2^{\bullet-}$, we designed a DA reaction between $C_6F_4I_2^{\bullet-}$ and 5-methyl-2-furoic acid in microdroplets (Figure 3a). The furoic acid was chosen instead of furan because

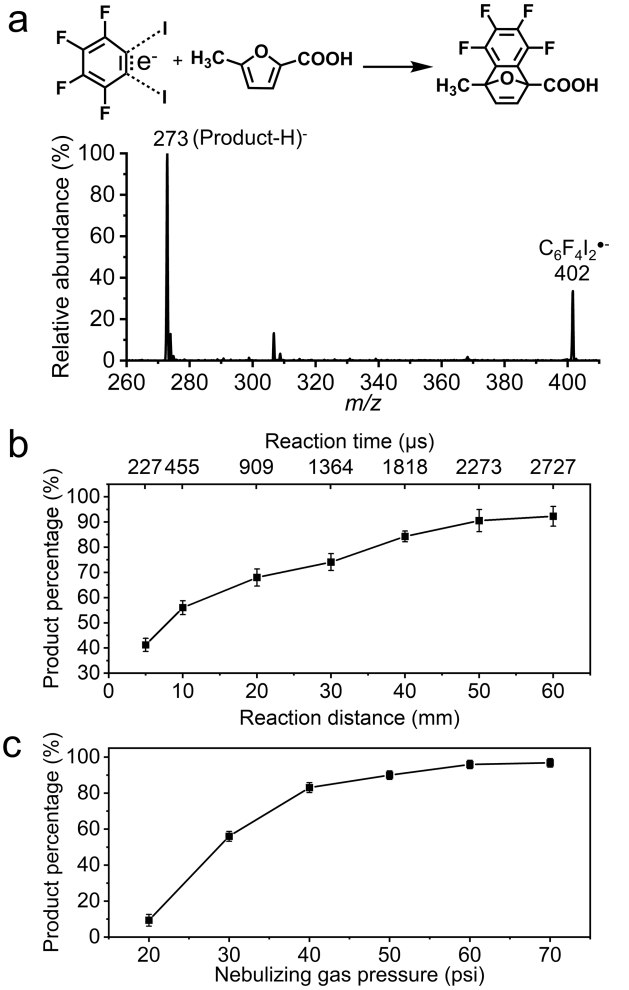

Figure 3. Microdroplet reaction between $C_6F_4I_2^{\bullet-}$ and 5-methyl-2-furoic acid. (a) Reaction and a typical mass spectrum showing the product. (b) Product percentage as a function of the reaction distance when the reactant concentrations are 200 μM and the sheath gas pressure is 30 psi. (c) Product percentage as a function of the sheath gas pressure when the reactant concentrations are 200 μM and the reaction distance is 10 mm.

deprotonation of the carboxylic acid could facilitate the easy mass spectrometric detection of the products. The mixed solution of $C_6F_4I_2$ and 5-methyl-2-furoic acid was sprayed into microdroplets. The deprotonated product peak is at m/z = 273.

Here, we define the product percentage as $I(\text{Product-H})^-/[I(\text{Product-H})^- + I(C_6F_4I_2^{\bullet-})]$, where I denotes the peak intensities. By adjusting the reaction distance from 5 to 60 mm, that is, to adjust the reaction time from 227 to 2727 μs,[39] a clear increase of the product percentage was observed (Figure 3b), indicating that the airborne microdroplet, but not the gas phase inside the mass spectrometer, was where the reaction occurs. To investigate the significance of the air−water interface of the microdroplets, we also monitored the product intensity when the sheath gas pressure was changed (Figure 3c). An increase in the product percentage was observed upon consecutively increasing the pressure from 20 to 70 psi, and

https://doi.org/10.1021/jacs.4c02819
J. Am. Chem. Soc. 2024, 146, 10979−10983

the product percentage exceeded 95% when the pressure reached 60 psi. Increasing the pressure decreases the sizes and increases the surface area to volume ratio of the droplets,[39] demonstrating the importance of the air−water interface for the reaction. The mass spectra in Figures S2 and S3 support the trends presented in Figure 3b,c, respectively. DFT simulation of the reaction between $C_6F_4I_2^{\bullet-}$ and furan shows a reaction barrier of only 14.6 kcal/mol (Figure S4), further supporting the DA reaction of the "quasi-benzyne".

3. CONCLUSIONS

To conclude, we have utilized the spontaneously generated electrons in water microdroplets to reduce $C_6F_4I_2$ into a $C_6F_4I_2^{\bullet-}$ radical anion, where the excess electron occupies the I−C1−C2−I bridge, which elongates the C−I bonds but shortens the C1−C2 bond. PES and DFT studies provided an atomic orbital level understanding of the unusual bond length change. Since the C1−C2 bond order in $C_6F_4I_2^{\bullet-}$ is higher than a double bond, it becomes similar to the benzyne molecule, as a result, we name it a "quasi-benzyne". The $C_6F_4I_2^{\bullet-}$ anion was further used for a DA reaction, a typical reaction for which the real benzyne molecule is well known. This study has pushed the limit of the microdroplet's ability of generating exotic anions via its reducing power. Since there are very few previous studies successfully applying furoic acid in DA reactions,[40] we anticipate that microdroplet chemistry can be an avenue rich in opportunities for new catalyst-free DA reactions involving biomass valorization.

■ ASSOCIATED CONTENT

Supporting Information

The Supporting Information is available free of charge at https://pubs.acs.org/doi/10.1021/jacs.4c02819.

Experimental and theoretical methods; additional experimental and theoretical results (PDF)

■ AUTHOR INFORMATION

Corresponding Authors

Kit Bowen − *Department of Chemistry, Johns Hopkins University, Baltimore, Maryland 21218, United States;* orcid.org/0000-0002-2858-6352; Email: kbowen@jhu.edu

Xinxing Zhang − *College of Chemistry, Key Laboratory of Advanced Energy Materials Chemistry (Ministry of Education), Renewable Energy Conversion and Storage Centre, Tianjin Key Laboratory of Biosensing and Molecular Recognition, Frontiers Science Centre for New Organic Matter, Nankai University, Tianjin 300071, China; Haihe Laboratory of Sustainable Chemical Transformations, Tianjin 300192, China;* orcid.org/0000-0001-5884-2727; Email: zhangxx@nankai.edu.cn

Authors

Huan Chen − *College of Chemistry, Key Laboratory of Advanced Energy Materials Chemistry (Ministry of Education), Renewable Energy Conversion and Storage Centre, Tianjin Key Laboratory of Biosensing and Molecular Recognition, Frontiers Science Centre for New Organic Matter, Nankai University, Tianjin 300071, China; Haihe Laboratory of Sustainable Chemical Transformations, Tianjin 300192, China*

Ruijing Wang − *College of Chemistry, Key Laboratory of Advanced Energy Materials Chemistry (Ministry of Education), Renewable Energy Conversion and Storage Centre, Tianjin Key Laboratory of Biosensing and Molecular Recognition, Frontiers Science Centre for New Organic Matter, Nankai University, Tianjin 300071, China; Haihe Laboratory of Sustainable Chemical Transformations, Tianjin 300192, China*

Tatsuya Chiba − *Department of Chemistry, Johns Hopkins University, Baltimore, Maryland 21218, United States*

Kathryn Foreman − *Department of Chemistry, Johns Hopkins University, Baltimore, Maryland 21218, United States*

Complete contact information is available at: https://pubs.acs.org/10.1021/jacs.4c02819

Author Contributions

‖H.C., R.W., and T.C. contribute equally.

Notes

The authors declare no competing financial interest.

■ ACKNOWLEDGMENTS

X.Z. acknowledges the National Key R&D Program of China (2023YFE0124200), the National Natural Science Foundation of China (22325402&22174073), the NSF of Tianjin City (21JCJQJC00010), the Haihe Laboratory of Sustainable Chemical Transformations, and the Frontiers Science Center for New Organic Matter at Nankai University (63181206). Part of this material (KHB) is based on work supported by the Air Force Office of Scientific Research (AFOSR) under grant number, FA9550-22-1-0271.

■ REFERENCES

(1) Yan, X.; Bain, R. M.; Cooks, R. G. Organic Reactions in Microdroplets: Reaction Acceleration Revealed by Mass Spectrometry. *Angew. Chem., Int. Ed.* **2016**, *55*, 12960−12972.

(2) Lee, J. K.; Banerjee, S.; Nam, H. G.; Zare, R. N. Acceleration of Reaction in Charged Microdroplets. *Q. Rev. Biophys.* **2015**, *48*, 437−444.

(3) Basuri, P.; Gonzalez, L. E.; Morato, N. M.; Pradeep, T.; Cooks, R. G. Accelerated Microdroplet Synthesis of Benzimidazoles by Nucleophilic Addition to Protonated Carboxylic Acids. *Chem. Sci.* **2020**, *11*, 12686−12694.

(4) Gao, D.; Jin, F.; Lee, J. K.; Zare, R. N. Aqueous Microdroplets Containing Only Ketones or Aldehydes Undergo Dakin and Baeyer-Villiger Reactions. *Chem. Sci.* **2019**, *10*, 10974−10978.

(5) Gnanamani, E.; Yan, X.; Zare, R. N. Chemoselective N-Alkylation of Indoles in Aqueous Microdroplets. *Angew. Chem., Int. Ed.* **2020**, *59*, 3069−3072.

(6) Wei, Z.; Li, Y.; Cooks, R. G.; Yan, X. Accelerated Reaction Kinetics in Microdroplets: Overview and Recent Developments. *Annu. Rev. Phys. Chem.* **2020**, *71*, 31−51.

(7) Banerjee, S.; Gnanamani, E.; Yan, X.; Zare, R. N. Can All Bulk-Phase Reactions be Accelerated in Microdroplets? *Analyst* **2017**, *142*, 1399−1402.

(8) Lee, J. K.; Walker, K. L.; Han, H. S.; Kang, J.; Prinz, F. B.; Waymouth, R. M.; Nam, H. G.; Zare, R. N. Spontaneous Generation of Hydrogen Peroxide from Aqueous Microdroplets. *Proc. Natl. Acad. Sci. U. S. A.* **2019**, *116*, 19294−19298.

(9) Li, L.; Xia, Y.; Song, X. W.; Chen, B. L.; Zare, R. N. Continuous Ammonia Synthesis from Water and Nitrogen via Contact Electrification. *Proc. Natl. Acad. Sci. U. S. A.* **2024**, *121*, No. e2318408121.

(10) Xiong, H.; Lee, J. K.; Zare, R. N.; Min, W. Strong Electric Field Observed at the Interface of Aqueous Microdroplets. *J. Phys. Chem. Lett.* **2020**, *11*, 7423−7428.

(11) Zhou, Z.; Yan, X.; Lai, Y. H.; Zare, R. N. Fluorescence Polarization Anisotropy in Microdroplets. *J. Phys. Chem. Lett.* **2018**, *9*, 2928−2932.
(12) Lhee, S. M.; Lee, J. K.; Kang, J.; Kato, S.; Kim, S.; Zare, R. N.; Nam, H. G. Spatial Localization of Charged Molecules by Salt Ions in Oil-Confined Water Microdroplets. *Sci. Adv.* **2020**, *6*, No. eaba0181.
(13) Xiong, H.; Lee, J. K.; Zare, R. N.; Min, W. Strong Concentration Enhancement of Molecules at the Interface of Aqueous Microdroplets. *J. Phys. Chem. B* **2020**, *124*, 9938−9944.
(14) Jin, S.; Chen, H.; Yuan, X.; Xing, D.; Wang, R.; Zhao, L.; Zhang, D.; Gong, C.; Zhu, C.; Gao, X.; Chen, Y.; Zhang, X. The Spontaneous Electron-Mediated Redox Processes on Sprayed Water Microdroplets. *JACS Au* **2023**, *3*, 1563−1571.
(15) Zhao, L.; Song, X.; Gong, C.; Zhang, D.; Wang, R.; Zare, R. N.; Zhang, X. Sprayed Water Microdroplets Containing Dissolved Pyridine Spontaneously Generate Pyridyl Anions. *Proc. Natl. Acad. Sci. U.S.A.* **2022**, *119*, No. e2200991119.
(16) Lee, J. K.; Samanta, D.; Nam, H. G.; Zare, R. N. Spontaneous Formation of Gold Nanostructures in Aqueous Microdroplets. *Nat. Commun.* **2018**, *9*, 1562.
(17) Gong, C.; Li, D.; Li, X.; Zhang, D.; Xing, D.; Zhao, L.; Yuan, X.; Zhang, X. Spontaneous Reduction-Induced Degradation of Viologen Compounds in Water Microdroplets and Its Inhibition by Host−Guest Complexation. *J. Am. Chem. Soc.* **2022**, *144*, 3510−3516.
(18) Chen, X.; Xia, Y.; Zhang, Z.; Hua, L.; Jia, X.; Wang, F.; Zare, R. N. Hydrocarbon Degradation by Contact with Anoxic Water Microdroplets. *J. Am. Chem. Soc.* **2023**, *145*, 21538−21545.
(19) Yuan, X.; Zhang, D.; Liang, C.; Zhang, X. Spontaneous Reduction of Transition Metal Ions by One Electron in Water Microdroplets and the Atmospheric Implications. *J. Am. Chem. Soc.* **2023**, *145*, 2800−2805.
(20) Chen, H.; Wang, R.; Xu, J.; Yuan, X.; Zhang, D.; Zhu, Z.; Marshall, M.; Bowen, K.; Zhang, X. Spontaneous Reduction by One Electron on Water Microdroplets Facilitates Direct Carboxylation with CO_2. *J. Am. Chem. Soc.* **2023**, *145*, 2647−2652.
(21) Hao, H.; Leven, I.; Head-Gordon, T. Can Electric Fields Drive Chemistry for an Aqueous Microdroplet? *Nat. Commun.* **2022**, *13*, 280.
(22) Chamberlayne, C. F.; Zare, R. N. Simple Model for the Electric Field and Spatial Distribution of Ions in a Microdroplet. *J. Chem. Phys.* **2020**, *152*, No. 184702.
(23) Heaney, H. The Benzyne and Related Intermediates. *Chem. Rev.* **1962**, *62*, 81.
(24) Zhang, B.; Wang, K. B.; Wang, W.; Wang, X.; Liu, F.; Zhu, J.; Shi, J.; Li, L. Y.; Han, H.; Xu, K.; Qiao, H. Y.; Zhang, X.; Jiao, R. H.; Houk, K. N.; Liang, Y.; Tan, R. X.; Ge, H. M. Enzyme-Catalysed [6 + 4] Cycloadditions in the Biosynthesis of Natural Products. *Nature* **2019**, *568*, 122−126.
(25) Gao, L.; Su, C.; Du, X.; Wang, R.; Chen, S.; Zhou, Y.; Liu, C.; Liu, X.; Tian, R.; Zhang, L.; Xie, K.; Chen, S.; Guo, Q.; Guo, L.; Hano, Y.; Shimazaki, M.; Minami, A.; Oikawa, H.; Huang, N.; Houk, K. N.; Huang, L.; Dai, J.; Lei, X. FAD-Dependent Enzyme-Catalysed Intermolecular [4 + 2] Cycloaddition in Natural Product Biosynthesis. *Nat. Chem.* **2020**, *12*, 620−628.
(26) Kurahashi, T.; Matsubara, S. Nickel-Catalyzed Reactions Directed toward the Formation of Heterocycles. *Acc. Chem. Res.* **2015**, *48*, 1703−1716.
(27) Hall, D. G.; Rybak, T.; Verdelet, T. Multicomponent Hetero-[4 + 2] Cycloaddition/Allylboration Reaction: From Natural Product Synthesis to Drug Discovery. *Acc. Chem. Res.* **2016**, *49*, 2489−2500.
(28) Haut, F. L.; Habiger, C.; Speck, K.; Wurst, K.; Mayer, P.; Korber, J. N.; Müller, T.; Magauer, T. Synthetic Entry to Polyfunctionalized Molecules through the [3 + 2]-Cycloaddition of Thiocarbonyl Ylides. *J. Am. Chem. Soc.* **2019**, *141*, 13352−13357.
(29) Vermeeren, P.; Hamlin, T. A.; Fernández, I.; Bickelhaupt, F. M. How Lewis Acids Catalyze Diels−Alder Reactions. *Angew. Chem., Int. Ed.* **2020**, *132*, 6260−6265.
(30) Shen, J.; Tan, C. H. Brønsted-Acid and Brønsted-Base Catalyzed Diels-Alder Reactions. *Org. Biomol. Chem.* **2008**, *6*, 3229−3236.
(31) Vermeeren, P.; Brinkhuis, F.; Hamlin, T. A.; Bickelhaupt, F. M. How Alkali Cations Catalyze Aromatic Diels-Alder Reactions. *Chem. Asian. J.* **2020**, *15*, 1167−1174.
(32) Chen, Q.; Gao, J.; Jamieson, C.; Liu, J.; Ohashi, M.; Bai, J.; Yan, D.; Liu, B.; Che, Y.; Wang, Y.; Houk, K. N.; Hu, Y. Enzymatic Intermolecular Hetero-Diels-Alder Reaction in the Biosynthesis of Tropolonic Sesquiterpenes. *J. Am. Chem. Soc.* **2019**, *141*, 14052−14056.
(33) Yang, C.; Liu, Z.; Li, Y.; Zhou, S.; Lu, C.; Guo, Y.; Ramirez, M.; Zhang, Q.; Li, Y.; Liu, Z.; Houk, K. N.; Zhang, D.; Guo, X. Electric Field-Catalyzed Single-Molecule Diels-Alder Reaction Dynamics. *Sci. Adv.* **2021**, *7*, No. eabf0689.
(34) Shaik, S.; Ramanan, R.; Danovich, D.; Mandal, D. Structure and Reactivity/Selectivity Control by Oriented-External Electric Fields. *Chem. Soc. Rev.* **2018**, *47*, 5125−5145.
(35) Aragones, A. C.; Haworth, N. L.; Darwish, N.; Ciampi, S.; Bloomfield, N. J.; Wallace, G. G.; Diez-Perez, I.; Coote, M. L. Electrostatic Catalysis of a Diels-Alder Reaction. *Nature* **2016**, *531*, 88−91.
(36) Zhang, D.; Lu, Y.; Wang, J.; Gong, C.; Hou, X.; Zhang, X.; Chen, J. Revisiting the Hitherto Elusive Cyclohexanehexone Molecule: Bulk Synthesis, Mass Spectrometry, and Theoretical Studies. *J. Phys. Chem. Lett.* **2021**, *12*, 9848−9852.
(37) Hanstorp, D.; Gustafsson, M. Determination of the Electron Affinity of Iodine. *J. Phys. B: At. Mol. Opt. Phys.* **1992**, *25*, 1773.
(38) Huang, K.; Leung, L.; Lim, T.; Ning, Z.; Polanyi, J. C. Single-Electron Induces Double-Reaction by Charge Delocalization. *J. Am. Chem. Soc.* **2013**, *135*, 6220−6225.
(39) Lai, Y.; Sathyamoorthi, S.; Bain, R. M.; Zare, R. N. Microdroplets Accelerate Ring Opening of Epoxides. *J. Am. Soc. Mass Spectrom.* **2018**, *29*, 1036−1043.
(40) Cioc, R. C.; Smak, T. J.; Crockatt, M.; van der Waal, J. C.; Bruijnincx, P. C. A. Furoic Acid and Derivatives as Atypical Dienes in Diels−Alder Reactions. *Green Chem.* **2021**, *23*, 5503−5510.

https://doi.org/10.1021/jacs.4c02819
J. Am. Chem. Soc. 2024, 146, 10979−10983